

Cooperative Multi-Agent Learning for Navigation via Structured State Abstraction

Mohamed K. Abdel-Aziz, *Graduate Student Member, IEEE*,

Mohammed S. Elbamby, *Member, IEEE*, Sumudu Samarakoon, *Member, IEEE*,

and Mehdi Bennis, *Fellow, IEEE*

Abstract

Cooperative multi-agent reinforcement learning (MARL) for navigation enables agents to cooperate to achieve their navigation goals. Using emergent communication, agents learn a communication protocol to coordinate and share information that is needed to achieve their navigation tasks. In emergent communication, symbols with no pre-specified usage rules are exchanged, in which the meaning and syntax emerge through training. Learning a navigation policy along with a communication protocol in a MARL environment is highly complex due to the huge state space to be explored. To cope with this complexity, this work proposes a novel neural network architecture, for jointly learning an adaptive state space abstraction and a communication protocol among agents participating in navigation tasks. The goal is to come up with an adaptive abstractor that significantly reduces the size of the state space to be explored, without degradation in the policy performance. Simulation results show that the proposed method reaches a better policy, in terms of achievable rewards, resulting in fewer training iterations compared to the case where raw states or fixed state abstraction are used. Moreover, it is shown that a communication protocol emerges during training which enables the agents to learn better policies within fewer training iterations.

M. K. Abdel-Aziz, and M. S. Elbamby are with Nokia Bell Labs, Espoo, Finland (e-mails: {mohamed.3.abdelaziz, mohammed.elbamby} @nokia-bell-labs.com).

S. Samarakoon, and M. Bennis are with the Centre for Wireless Communications, University of Oulu, Oulu, Finland (e-mails: firstname.lastname@oulu.fi).

M. K. Abdel-Aziz contributed to this work while being with the Centre for Wireless Communications, University of Oulu.

Index Terms

Reinforcement learning, emergent communication, multiagent, state abstraction, structure, graph neural network, quadtree, adaptive.

I. INTRODUCTION

Shannon and Weaver categorized communication problems into three levels [1]: *Level A* asks the question of how accurately can the communication symbols be transmitted (The technical problem), while *Level B* asks the question of how precisely do the transmitted symbols convey the desired meaning (The semantic problem), and finally *Level C* asks the question of how effectively does the received meaning affect conduct in the desired way (The effectiveness problem). Beyond Shannon communication regimes tackle both the semantic and effectiveness problems (levels B and C). One possible area that could benefit from solving such problems is cooperative multi-agent navigation.

Recently, automated guided vehicles (AGVs) have been successfully deployed owing to their increased productivity and scale to support automation processes [2]. Therein, vehicles' navigation capabilities, specifically field-of-view (FoV)-based navigation, is a crucial problem [3]. Fundamentally, FoV-based navigation is a task where a group of vehicles (also referred to as agents) aims at reaching an unknown destination by utilizing their local sensory information. One traditional framework to solve such navigation tasks is by combining multiple modules, such as simultaneous localization and mapping (SLAM) [4], [5], path planning [6], and so forth. According to [3], integrating such modules in practical applications involves large computational errors, leading to poor performance. Moreover, a high-precision global map is required for such a traditional framework, resulting in limitations in navigating in unknown or dynamic environments. With the remarkable capabilities of deep learning technology, deep reinforcement learning (DRL) has been used to directly learn navigation strategies from raw sensory inputs [3], [7], [8]. In [7], a target-driven concept is proposed where the DRL algorithm is found to be generalizable to new scenarios, but at the expense of a decrease in performance. While in [8], a new neural network architecture was proposed in order to jointly learn a navigation task via

RL along with additional auxiliary tasks. However, this approach was found to have an unstable policy and poor robustness in a complex environment [3].

In particular, DRL has proved to be a powerful tool in goal-directed learning and complex decision-making scenarios. DRL is best utilized when a single agent is learning from interactions how to behave in an environment in order to achieve a certain goal or task, notably when the state space is huge [9].

However, DRL agents must learn about their environment through high-dimensional noisy local observations, while receiving sparse or delayed rewards. Individually solving the FoV-based navigation task by each agent¹ is challenging due to the partial observation of the environment, i.e., each agent only utilizes local sensory information to achieve the task, leading to a complicated learning behavior. As a result, multiple agents need to cooperate in order to achieve their goals. This cooperation and interaction between multiple simultaneously learning agents in the same environment is referred to as multi-agent reinforcement learning (MARL) [10], [11]. There have been plenty of works utilizing MARL to solve complex FoV-based navigation tasks [12]–[14].

In cooperative MARL environments, agents utilize communication protocols to cooperate and coordinate. However, manually designing such a protocol within a cooperative MARL environment is a daunting task, due to the large number of states and partial (and often noisy) information available for each agent. Moreover, the resulting protocol may not necessarily be optimal for the given task [15]. Alternatively, agents could learn communication protocols to coordinate and share information that is needed to complete the tasks in a much faster and robust manner [16]. Learning a communication protocol in an MARL environment is referred to as emergent communication. In this setting, communication is emergent in the sense that, at the beginning of training, the symbols emitted by the agents have no predefined semantics nor pre-specified usage rules. Instead, the meaning and syntax emerge through training [17].

Nonetheless, having multiple learning agents within the same environment poses an extra challenge to the learning problem as the problem’s complexity increases exponentially with the number of agents [10]. According to [10], [18], DRL and MARL usually require millions of

¹agent, vehicle, and robot are used interchangeably throughout the paper.

interactions for an agent to learn, due to the huge state space that needs to be explored to learn a suitable policy. Moreover, learning a communication protocol on top of that deteriorates the exploration problem because the state space grows even more with the added communication, and the likelihood for a consistent protocol to be found becomes difficult [19].

Traditionally, the huge state space problem in modern RL tasks is tackled by function approximation schemes, such as, by using deep neural networks to approximate the value and/or policy functions. Those function approximation schemes are often employed to provide a compact representation so that RL can generalize across states. Empirically, combining various RL function approximation algorithms with neural networks for feature extraction has led to immense successes in various tasks [9], [20], [21]. However, as mentioned earlier, these methods often require a large number of samples to learn a good policy [10], [18]. Another approach to tackle the huge state space problem is via state abstraction. State abstraction is a method for compressing the environment’s state space to transform complex problems into simpler ones with more compact forms [22]. Abstraction gives rise to models of the environment that are compressed and useful for downstream tasks, enabling efficient training, decision making and generalization. The state abstraction problem was tackled previously in [22], where the authors formulated and analysed the trade-off between abstraction and RL performance. Therein, the knowledge of the expert RL policy was assumed a priori. This expert policy is then used for learning *state abstractions*. Further, the size of the abstracted space was determined a priori. Finally, in order to allow agents to learn concepts from data, the state space needs to be structured [23], so that agents can generalize better to new environments not seen during training.

A. Contributions

In this work, we propose a novel neural network architecture to jointly learn adaptive state space abstraction strategies, along with a communication protocol among agents, with a specific emphasis on a FoV-based cooperative navigation scenario. The main goal of the adaptive abstractor is to determine a suitable state abstraction based on the learnt communication protocol, which reduces the size of the state space to be explored (the semantic problem), which in turn helps the agents achieve their goal, without much degradation in the policy performance (the

effectiveness problem). Unlike [22], the proposed approach does not assume any prior knowledge of an expert policy to learn the abstraction. Moreover, the size of the abstracted space is not determined a priori. For the FoV-based navigation scenario studied in this work, a structured state of the environment is obtained by utilizing the Quad/Octree decomposition method [24]. Simulation results show that the proposed method reaches a better policy, in terms of achievable rewards in less number of training iterations, compared to the case when raw states are used for policy learning, or when a fixed state abstraction is used. Moreover, it is shown that the trained policy can generalize to cases when the local observations are uncertain about up to 60% of its local information due to noise, distortions, or obstructed views.

Finally, it is shown that a communication protocol emerges during training which helps the agents learn better policies within fewer training iterations.

The rest of this paper is organized as follows. In Section II, the system model is introduced. The problem is formulated in Section III. In Section IV, the proposed adaptive abstractor is presented followed by the training process. Finally, the simulation setup and results are discussed in Section V, while conclusions are drawn in Section VI.

II. SYSTEM MODEL

As shown in Fig. 1, we consider N autonomous agents navigating in a grid world of size $L \times L$. This grid world has one green goal and several obstacles with the density of ϱ . We assume that each agent n knows its current location l_n within the grid world. Additionally, each agent observes a partial view of the environment, of size $M \times M$, centered at its current location, where $M < L$, and M is assumed to be a power of 2. Moreover, agents cannot see through the obstacles. As a result, from any agent's perspective, the state at any location on the grid within the agent's FoV can be one of three cases:

- Occupied (s_+): If an obstacle is sensed at that location.
- Unoccupied (s_-): If the location is obstacle-free.
- Unknown (s_0): If the location falls within the agent's blind spot, e.g., behind an obstacle.

Furthermore, to promote cooperation between agents, each agent is given access to a control channel to broadcast communication symbols to neighboring agents. In particular, each agent

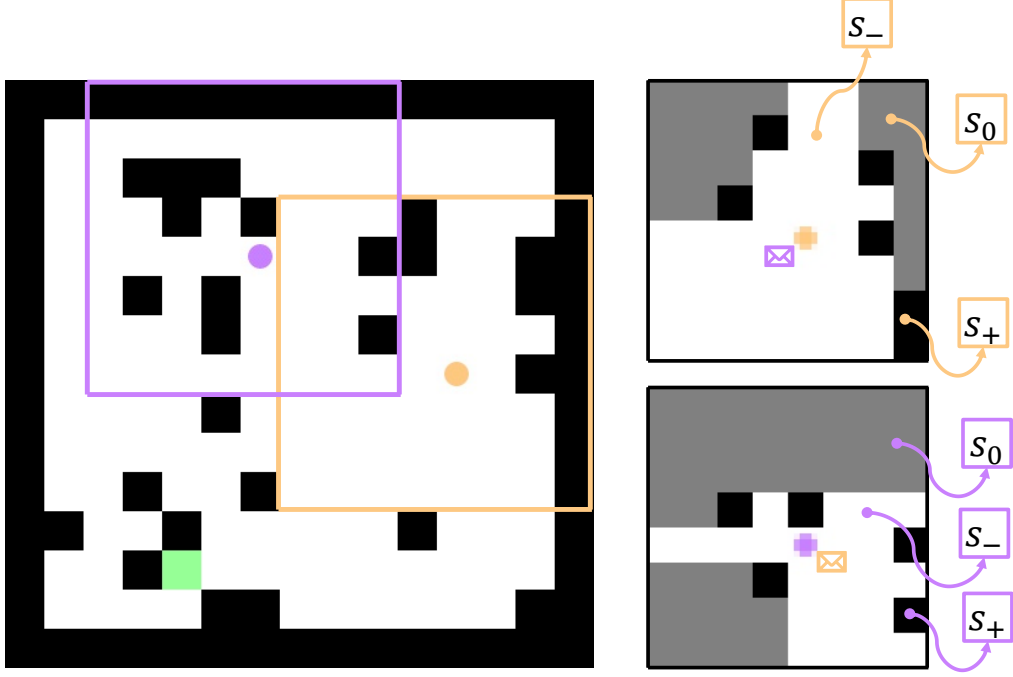


Figure 1: A 15×15 grid world (left) with obstacles (black tiles) and two agents (circles) having a partial observation of size 8×8 . Agents cooperatively navigate to the destination (green tile) by only utilizing their partial observation and communicated symbols (right).

n maintains a vocabulary \mathcal{C}^n of size C , i.e., $|\mathcal{C}^n| = C$. These communication symbols $c \in \mathcal{C}^n$ have no predefined semantics, nor pre-specified usage rules [17]. Instead, the agents should learn how to utilize these symbols while solving the navigation task, resulting in an emergence of a communication protocol. Here, the cooperative objective of the agents is to navigate to the green goal location, by only utilizing their local partial observation and via communication leveraging the control channel.

III. PROBLEM FORMULATION

The cooperative navigation task can be viewed as an MARL task with communication, which is modeled as a partially observable general-sum Markov game [19], [25]. Each agent obtains a partial observation of the global state at every time step. This partial observation includes the agent's current location, and the $M \times M$ partial view of the environment. This observation, along with all symbols communicated on the control channel, is used to learn a policy that maximizes

the agent's reward. A reward of 1 is received by each agent that completes the task. A deep neural network is used to parameterize the policy function.

Formally, a decentralized MARL can be described as a partially observable Markov decision process (POMDP), $\langle N, \mathcal{S}, \mathcal{A}, \mathcal{C}, \mathcal{O}, \mathcal{T}, R, \gamma \rangle$, where N is the number of agents, \mathcal{S} is the global state space, $\mathcal{A} = \{\mathcal{A}^1, \dots, \mathcal{A}^N\}$, $\mathcal{C} = \{\mathcal{C}^1, \dots, \mathcal{C}^N\}$, and $\mathcal{O} = \{\mathcal{O}^1, \dots, \mathcal{O}^N\}$ are sets of actions, communications, and observation spaces, respectively.

At time-step t , each agent n obtains a partial observation $o_t^{(n)} \in \mathcal{O}^n$ of the global state s_t , and a set of communicated symbols from the previous time step $c_{t-1} = \{c_{t-1}^{(1)}, \dots, c_{t-1}^{(N)}\}$. The agent then selects an action $a_t^{(n)} \in \mathcal{A}^n$ and a communication symbol to broadcast $c_t^{(n)} \in \mathcal{C}^n$. Given the joint actions of all agents $a_t = \{a_t^{(1)}, \dots, a_t^{(N)}\}$, the transition function $\mathcal{T} : \mathcal{S} \times \mathcal{A}^1 \times \dots \times \mathcal{A}^N \rightarrow \Delta(\mathcal{S})$ maps the current state s_t and set of actions a_t to $\Delta(\mathcal{S})$, a probability distribution over the next state s_{t+1} . Finally, each agent receives an individual reward $r_t^{(n)} \in R(s_t, a_t)$ where $R : \mathcal{S} \times \mathcal{A}^1 \times \dots \times \mathcal{A}^N \rightarrow \mathbb{R}$. A fully cooperative setting is considered for this task, where the objective of each agent is to maximize the total expected return of all agents:

$$\underset{\pi: \mathcal{S} \rightarrow \mathcal{A} \times \mathcal{C}}{\text{maximize}} \quad \mathbb{E} \left[\sum_{t \in T} \sum_{n \in N} \gamma^t R(s_t, a_t) \quad \middle| \quad (a_t, c_t) \sim \pi^{(n)}, s_t \sim \mathcal{T}(s_{t-1}) \right], \quad (1)$$

for some finite time horizon T and discount factor γ .

In MARL, (1) is optimized using policy gradient [19]. Here, any policy optimization algorithm can be used to optimize the policy network. However, directly using raw pixel observations as states poses a huge challenge for the learning problem. This is due to the unstructured nature of pixel data [19], as well as the huge observation space that needs to be explored to optimize the policy network [10].

To overcome those pressing challenges, a structured-state abstraction is leveraged. State abstraction is a method for simplifying complex problems into simpler forms by compressing the state space into a structure-preserving manner [22], [23]. State abstraction could be carried out by eliminating unimportant states or combining states into groups to create a smaller state space [26]. However, if abstraction compresses too much information, this would affect the agent's performance. Thus, care must be taken to identify the optimal state abstraction that balances

between an appropriate degree of compression and acceptable representational power. Moreover, if the state space is structured, this allows the agent to form concepts by forming equivalent classes, and use them for better generalization [23].

In order to carry out state abstraction, the unstructured raw pixel observations can be transformed into a structured observation space by utilizing the concept of region quadtree decomposition [24]². Quadtree is a tree data structure used to efficiently store and represent two-dimensional space data, e.g., $M \times M$ partial view of the environment observed by each agent. A quadtree decomposition recursively decomposes a two-dimensional space into four equal sub-regions till all the locations within a sub-region have the same state or until reaching a maximum predefined resolution (tree-depth). Moreover, a full-resolution quadtree is defined as a quadtree that is decomposed until the finest granularity is reached.

A quadtree can be modeled as an unweighted graph $G = (\mathcal{V}, \mathcal{E})$ where \mathcal{V} is the set of nodes in the quadtree and \mathcal{E} is the set of branches. Moreover, each node $v \in \mathcal{V}$ has a feature vector X_v that consists of the node index as well as its state. Fig. 2 shows different levels of quadtree representations of the agent’s partial observation.

Abstracting the resultant quadtree structure can now be done by adaptively trimming branches of the quadtree structure. For abstraction to be deemed useful and to enhance the agent’s performance, abstraction should be a function of the agent’s partial observation and the communication symbols received from other agents. In this paper, we propose a local adaptive abstractor at each agent that learns which quadtree branches to trim (abstracting the state space) depending on the current partial observation and received communication symbols. Note that the communicated symbols will guide the abstraction process, depending on how they are interpreted by the agents.

IV. PROPOSED ADAPTIVE ABTRACTOR AND TRAINING PROCESS

In order to learn which quadtree branches to trim without affecting the agent’s policy performance, we propose a neural network architecture for learning the abstractor. Here, the abstractor neural network uses the full-resolution quadtree of the agent’s $M \times M$ partial view of the environment, its current location, and the received communication symbols as input and then

²If 3D observation is available, Octree decomposition [24] could be utilized without any changes to the proposed solution.

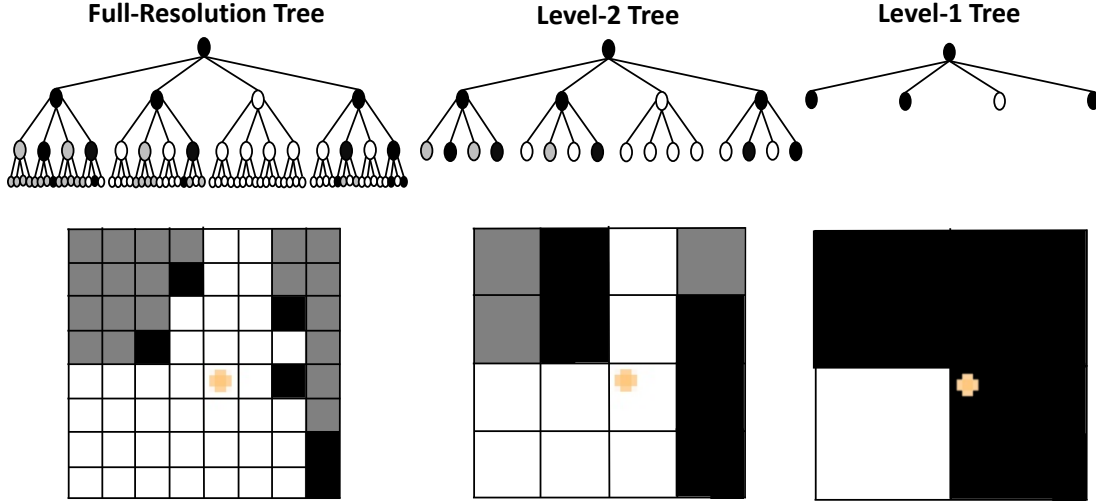


Figure 2: Different levels of quadtree representation (top) with the corresponding observations (bottom).

outputs the trimmed quadtree structure. This output along with the communicated symbols is then used to learn a policy that maximizes the agent’s reward. As mentioned earlier, abstraction reduces the size of the observation space to be explored during policy learning, without much degradation in the policy performance. The proposed neural network architecture of the abstractor is presented in Fig. 3. The details of each component will be discussed in the following subsections.

A. Graph Isomorphism Network

Learning with graph structured data, such as quadtrees, demands an effective representation of this structure [27]. Representation learning of such graph structures is made possible by graph neural networks (GNNs). GNNs utilize the graph structure and node features to learn a representation (or an embedding) of the entire graph. GNNs follow a neighbourhood aggregation strategy where the representation of a node is iteratively updated by aggregating representations of its neighbours. After the k ’s iteration, a node’s representation captures structural information within its k -hop network neighbourhood. At the final iteration K , a readout function aggregates the representations of the nodes to obtain the entire graph’s representation h_G . The k -th and

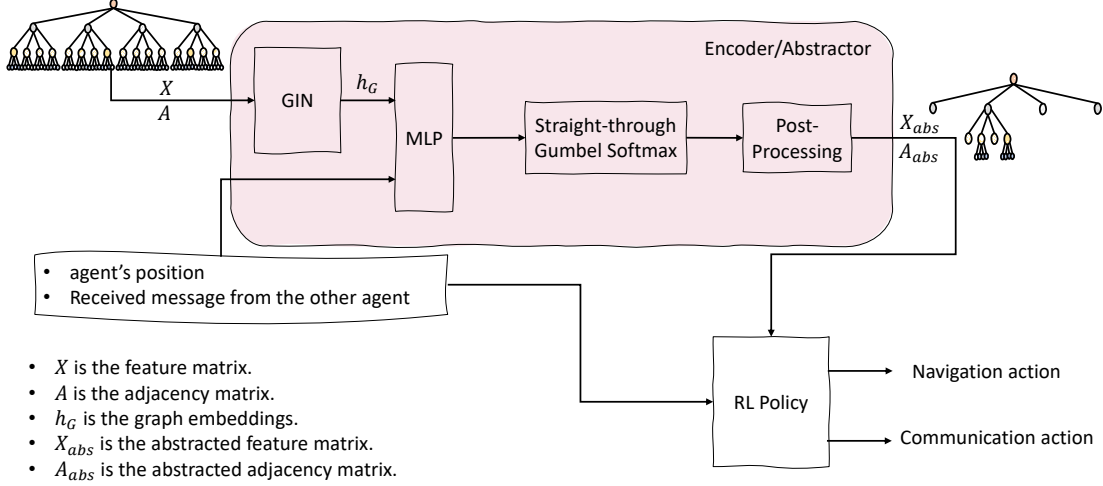


Figure 3: Neural network architecture of the proposed abstractor at each agent.

final iteration K of a GNN can be represented as follows:

$$b_v^{(k)} = \text{AGGREGATE}^{(k)} \left(\{h_u^{(k-1)} : u \in \mathcal{N}(v)\} \right), \quad (2)$$

$$h_v^{(k)} = \text{COMBINE}^{(k)} \left(h_v^{(k-1)}, b_v^{(k)} \right), \quad (3)$$

$$h_G = \text{READOUT} \left(\{h_v^{(K)} \mid v \in G\} \right) \quad (4)$$

where $h_v^{(k)}$ is the feature vector of node v at the k -th iteration³, and $\mathcal{N}(v)$ is the set of nodes adjacent to v . Fig. 4 illustrates the GNN operations. The choice of $\text{AGGREGATE}^{(k)}$, $\text{COMBINE}^{(k)}$, and READOUT functions in GNNs is crucial [27].

For the GNN to have maximal representational power and disambiguate between different graph structures, i.e., by mapping them to different representations, the $\text{AGGREGATE}^{(k)}$, $\text{COMBINE}^{(k)}$, and READOUT functions need to be injective [27]. As a result, graph isomorphism network (GIN) represents (3) and (4) as follows:

$$h_v^{(k)} = \text{MLP}^{(k)} \left(h_v^{(k-1)} + \sum_{u \in \mathcal{N}(v)} h_u^{(k-1)} \right), \quad (5)$$

$$h_G = \text{CONCAT} \left(\sum_{v \in G} h_v^{(k)} \mid k = 0, 1, \dots, K \right). \quad (6)$$

³ $h_v^{(0)}$ is initialized to the node features X_v .

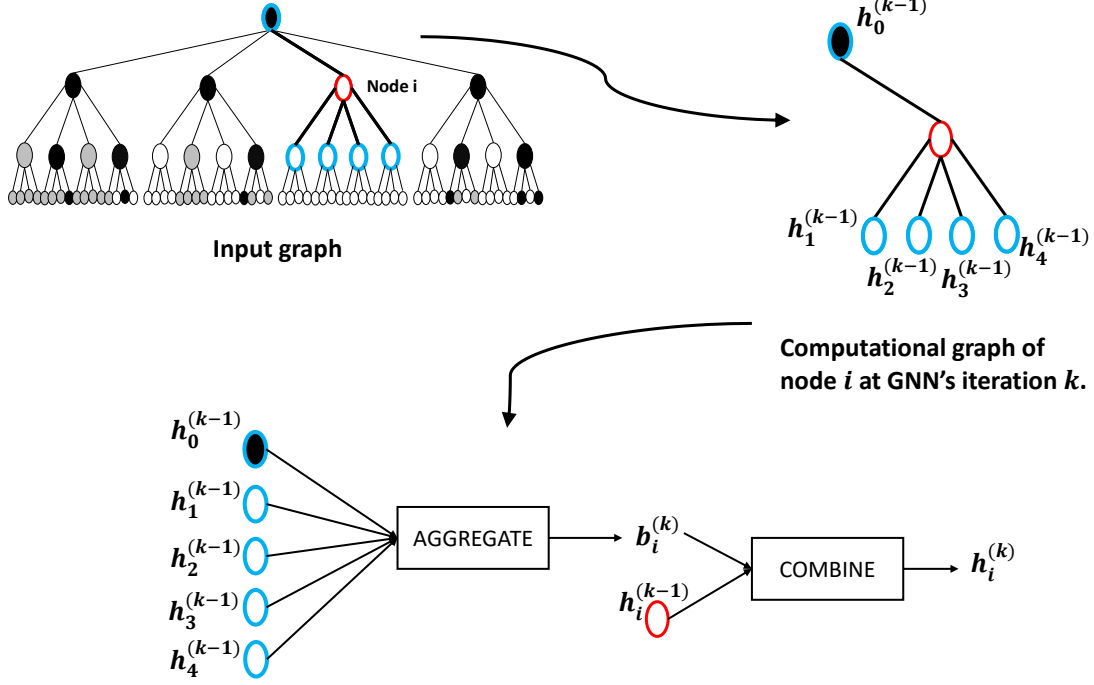


Figure 4: An illustration of the k^{th} iteration (or layer) of a general GNN model.

where MLP is a multi-layer perceptron, and CONCAT is the concatenation function.

Due to its representational power that could distinguish between different structures by mapping them to different representations⁴, GIN is utilized in our proposed architecture. As a summary, the input of the GIN in our framework is the full-resolution tree represented as (i) the feature matrix X which includes the feature vector of each node in the quadtree, and (ii) the adjacency matrix A where an entry a_{ij} is equal to 1 only if there is a branch (or edge) between node i and node j in the quadtree structure. Otherwise it is equal to 0. The output of the GIN is the entire graph's representation h_G .

B. MLP and Straight-through Gumbel softmax

After obtaining the graph representation h_G , it needs to be combined with the other information available at the agent, specifically, the agent's location and the received communication symbols from the previous time slot. This combining is done by concatenating all these information and

⁴The ability to map any two different structures to different embeddings entails solving the graph isomorphism problem. For more details, please refer to [27].

passing them to an MLP. Note that, the internal nodes⁵ of the input tree-structure are the nodes that could be merged. As a result, the output of the MLP is set to be $2 \times |\mathcal{V}^*|$, where \mathcal{V}^* is the set of internal nodes. The reason behind this is to compute a merge and non-merge score for each internal node and sample according to this score by utilizing straight-through Gumbel-softmax estimator (ST-GS) [28]. ST-GS uses the argmax operator over Gumbel random variables to generate a discrete random outcome in the forward pass and it maintains differentiability in the backward pass. The detailed information about the ST-GS estimator can be found in [28]. The output of ST-GS in the forward pass is a binary vector yielding the merging decision of each internal node.

C. Post processing

If the abstractor decides to merge a certain node, then all of its children should be discarded from the feature matrix X , and the adjacency matrix A . This will result in the abstracted (or trimmed) tree represented by the abstracted feature matrix X_{abs} and the abstracted adjacency matrix A_{abs} .

D. Decentralized training process

In this work, decentralized training is considered, where each agent is parameterized by an independent policy. As mentioned earlier, any policy optimization algorithm could be used to optimize the policy network.

Since no expert policy is assumed to be known, the training of the abstractor is carried out simultaneously while training and optimizing the policy network. The training objective is to minimize the number of branches within the input tree, while still being able to complete the assigned task. Specifically, during training, the agent minimizes the following loss function \mathbb{L} :

$$\mathbb{L} = \mathbb{L}_{\text{RL}} + \|A_{\text{abs}}\|_{\text{F}}, \quad (7)$$

where \mathbb{L}_{RL} is the RL loss dependent on the chosen policy optimization algorithm, and $\|A_{\text{abs}}\|_{\text{F}} = \sqrt{\sum_{i,j} |a_{ij}|^2}$ is the Frobenius norm of A_{abs} . In this work, we use asynchronous advantage actor-

⁵Internal nodes are the nodes of the quadtree that are neither a root nor a leaf.

critic (A3C) [29] to optimize the agent’s policy network, similar to [19]. A3C is an actor-critic policy gradient algorithm that uses multiple CPU threads on a single machine. This would allow for a reduction in training time, as well as a stabilization in the learning process without the need for an experience replay [29]. Since A3C is out of scope of this work, we refer interested readers to [29] for more details on the training algorithm.

V. SIMULATION SETUP AND ANALYSIS

In this section, we demonstrate the benefits of the proposed abstractor compared to several baselines. The evaluation is done in an environment called `FindGoal`, adopted from [19]. A snapshot of this environment is shown in Fig. 1. In `FindGoal`, the task is to reach the green goal location. Each agent receives a reward of 1 when they reach the goal. It should be noted that the states of the environment, e.g., locations of agents, goal and obstacles are randomized at every episode. Specifically, the map is a 15×15 grid world. At the beginning of each episode, a single goal tile and 25 obstacle tiles are randomly placed on the map. Then, two agents are randomly placed on the remaining empty space. Each agent can only observe an 8×8 partial view of the map centered on the agent. Each agent has five actions: up, down, left, right, and stay. The maximum episode length allowed is 1024 time steps. More simulation parameters are detailed in Table I. For all simulations, the Adam optimizer [30] is used with a learning rate of 0.0001 and parameters $\beta_1 = 0.9$, $\beta_2 = 0.999$, $\epsilon = 10^{-8}$.

A. Baselines

We compare the proposed adaptive abstractor to four baselines detailed as follows:

- **Full Resolution Image:** In this baseline, the local view of the agent, as in Fig. 1, is processed using a convolutional neural network (CNN), and the output is passed to the RL policy, along with the agent’s position and the received symbol from the other agent.
- **Full Resolution Tree:** In this baseline, the full resolution image is decomposed into the full-resolution quadtree, as shown in Fig. 2. The full-resolution quadtree, represented by its feature matrix and adjacency matrix, is processed by GNN without using the abstractor. The

Table I: Simulation parameters

Parameter	Value	Parameter	Value
L	15	ϱ	0.15
M	8	C	1024
N	2	γ	0.99
K	5	T	1024

output is passed to the RL policy, along with the agent’s position and the received symbol from the other agent.

- **Level-2 Tree:** Here, the full resolution image is decomposed into the level-2 quadtree, as shown in Fig. 2. This tree, represented by its feature matrix and adjacency matrix, is processed by GNN, and the output is passed to the RL policy, along with the agent’s position and the received symbol from the other agent.
- **Level-1 Tree:** Here, the full resolution image is decomposed into the level-1 quadtree, as shown in Fig. 2. This tree, represented by its feature matrix and adjacency matrix, is processed by GNN, and the output is passed to the RL policy, along with the agent’s position and the received symbol from the other agent.

Level-1/level-2 tree can be seen as the output of a fixed abstractor that always abstract the quadtree to the first/second level in contrast to the proposed abstractor that adaptively trim branches of the quadtree depending on the system state.

B. Training performance evaluation

First of all, in Figs. 5, 6, and 7, we evaluate the training speed and the performance of the trained policy using the proposed adaptive abstractor (**Proposed**), and compare it with the four baselines outlined earlier.

Figs. 5 and 6 show the reward achieved by each agent throughout training. The faded background curves are the actual achieved reward, where each point over these curves is the average reward over 10 evaluation episodes. These curves are smoothed, to gain insights about the training process, by a moving average over a window size of 200 000 training iterations (or episodes). The smoothed curves are represented by solid lines. We observe that the baselines

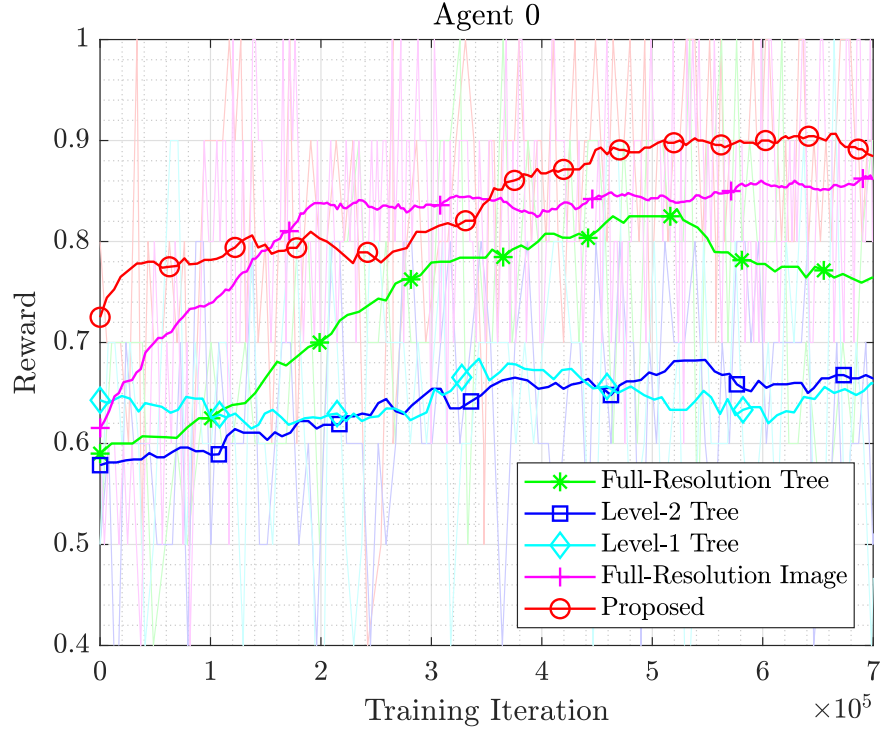


Figure 5: The reward achieved by agent 0 throughout training.

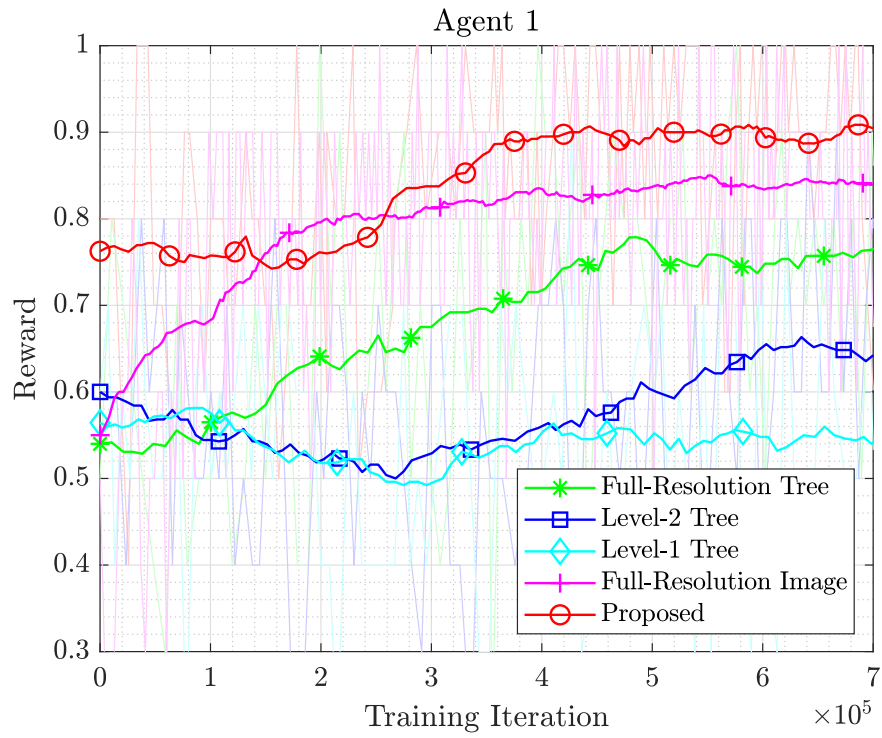


Figure 6: The reward achieved by agent 1 throughout training.

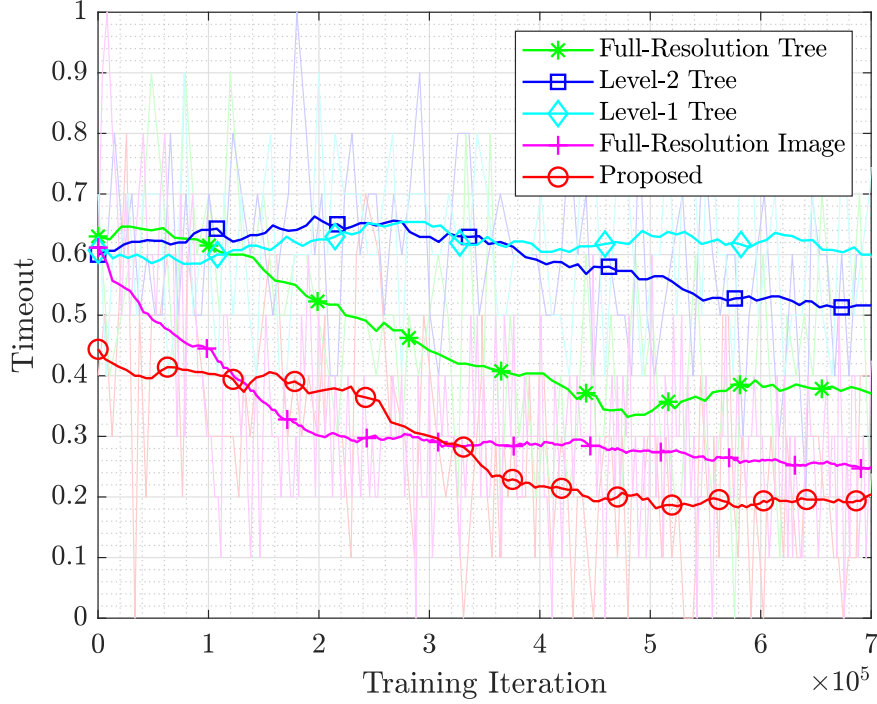


Figure 7: Timeout during the evaluation episodes throughout training.

with fixed abstractions, e.g., **Level-1 Tree** and **Level-2 Tree**, fail to learn good policies during training. This is due to the loss of useful information under abstraction that neglects the current observation and the received communication symbols from the other agent. It can be noted that the adaptive abstraction (**Proposed**) method learns a policy that has better performance in terms of the achieved reward compared to **Full-Resolution Image** and **Full-Resolution Tree** baselines, although these baselines utilize all the available information without any abstraction. This can be attributed to the adaptive capability of the proposed abstractor that trims the input tree depending on the current observation and the received communication symbols, which yields a low-complexity yet informative tree structure. Hence, the state space to be explored is reduced resulting in faster and better learning compared to the full-resolution baselines.

Fig. 7 shows the rate of failure of the agents during the evaluation episodes throughout the training process. Here, an episode is considered as a failure if any of the agents did not reach the goal location within the allowed maximum episode length. The fraction of failures compared to total episodes is defined as the rate of failure, which is referred to as **Timeout** hereinafter. Similar

to Figs. 5 and 6, the background curves are the achieved reward over short intervals, where each point corresponds to the average reward over ten evaluation episodes. These curves are smoothed by the moving average over a window size of 200 000 training iteration (or episode) and represented by the solid lines. We notice the same trend in the performance as with the achieved reward by the agents, where the proposed adaptive abstractor outperforms the baselines and achieves a lower timeout after fewer training iterations. This is due to the abstractor’s capability of extracting low-complexity yet informative tree structures, as discussed under the results of Figs. 5 and 6.

C. Abstraction

One of the compelling question we want to address is “how much abstraction is achieved using the proposed adaptive abstractor?”. In order to measure the degree of abstraction, we resort to $\|A\|_F = \sqrt{\sum_{i,j} |a_{ij}|^2}$, which is directly proportional to the tree size.

The tree size of the proposed adaptive abstractor during the training process along with the tree sizes of the tree-based baselines: **Full-Resolution Tree**, **Level-1 Tree**, and **Level-2 Tree** are presented in Fig. 8. Since the tree-based baselines can be considered as approaches with fixed abstraction, their tree sizes are represented by straight lines. Note that, the size of the tree achieved by the proposed method lies between **Level-1** and **Level-2** trees. Despite of that, the trained policy using the proposed abstractor outperforms that of the baselines, as shown in Section V-B. This can be attributed to the adaptive capability of the abstractor that trims the input tree as a function of the agent’s local information and received message while preserving the useful information.

D. Generalization

In order to evaluate the generalization aspects of the trained policy, we adopt new situations where the local observation of each agent is distorted with noise. The noisy observations are characterized by a noise level α . Specifically, during evaluation, the occupied s_+ and unoccupied s_- states of the locations within an agent’s FoV are observed correctly by the agent with probability $1 - \alpha$, and are seen as unknown states s_0 with probability α . This scenario models

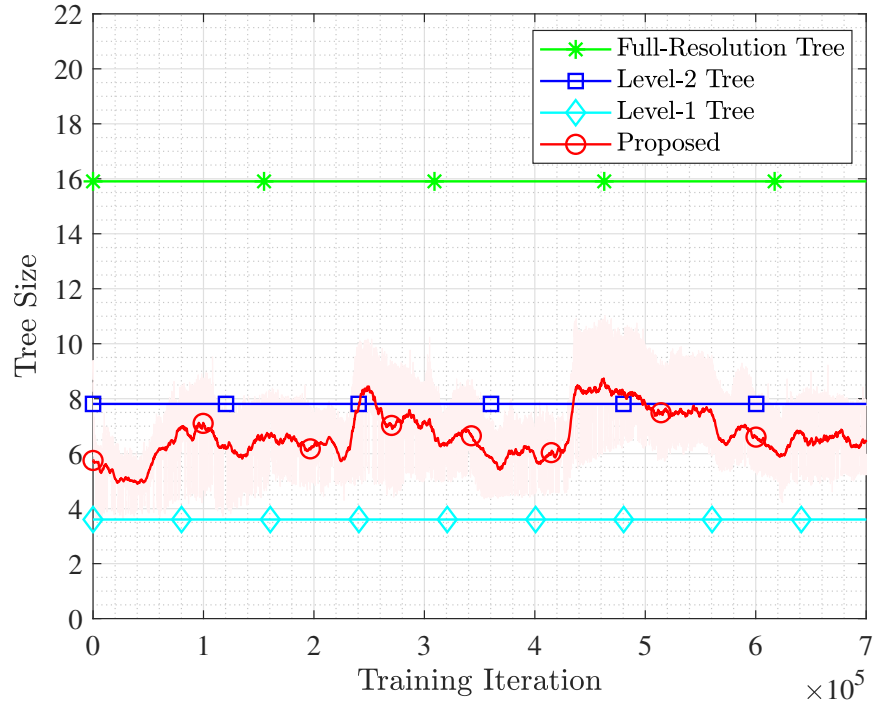


Figure 8: Size of the tree during the training process.

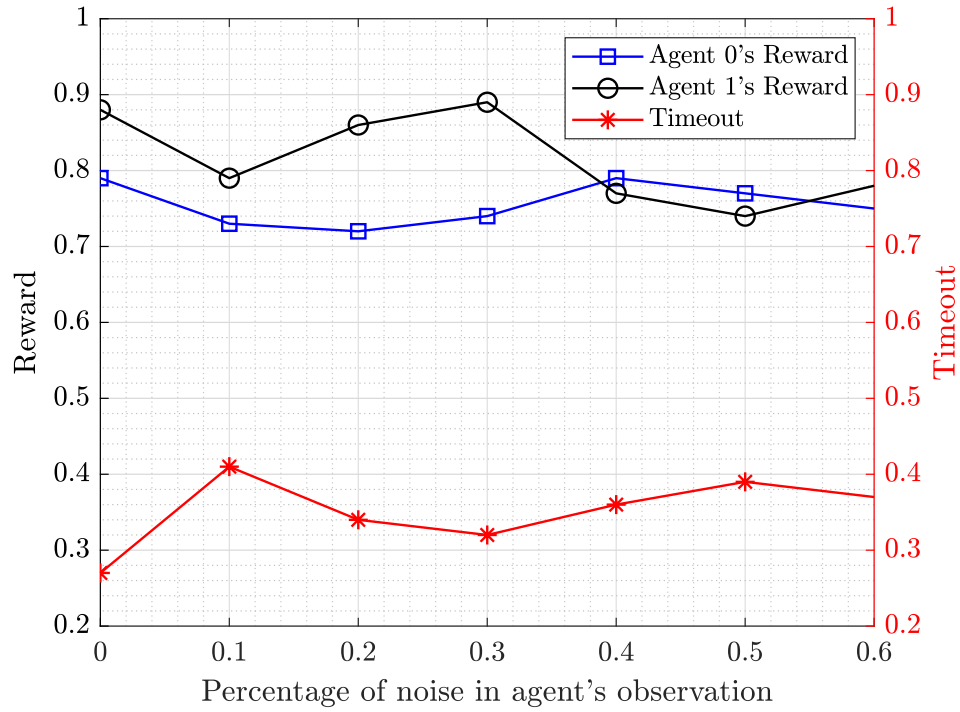


Figure 9: Reward and timeout achieved by a trained policy over different values of noise probability levels α .

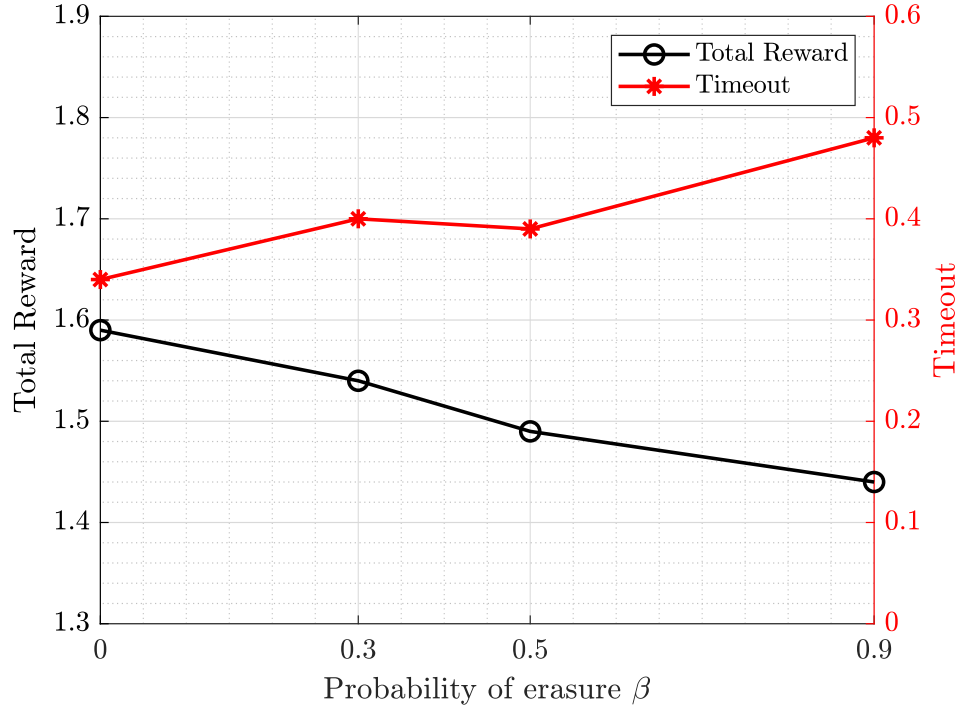


Figure 10: Total reward and timeout achieved by a trained policy over different values of channel erasure probability β .

the practical case where sensors on a deployed agent are worn out or noisy, thereby affecting the agent’s local observation and navigation task.

We run 100 evaluation episodes utilizing the trained policies for different values of α . Fig. 9 shows the achieved performance where each point is the average over 100 evaluation episodes. Note that the policy is trained in noise-free setting, i.e., with $\alpha = 0$. We observe that the policy generalizes well with only a small degradation in performance, even when $\alpha = 0.6$. This can be attributed to the structured input space, which allows the agent to see similarities and form concepts, enabling the agent to generalize better [23].

Moreover, in order to assess the sensitivity of the trained policy to link level quality, we evaluate the trained agents in an environment with erasure channels. In such environment, the symbols transmitted over these channels can be erased with a certain probability β , and can be received correctly with probability $1 - \beta$.

We run 100 evaluation episodes utilizing the trained policies for different values of β . Fig. 10

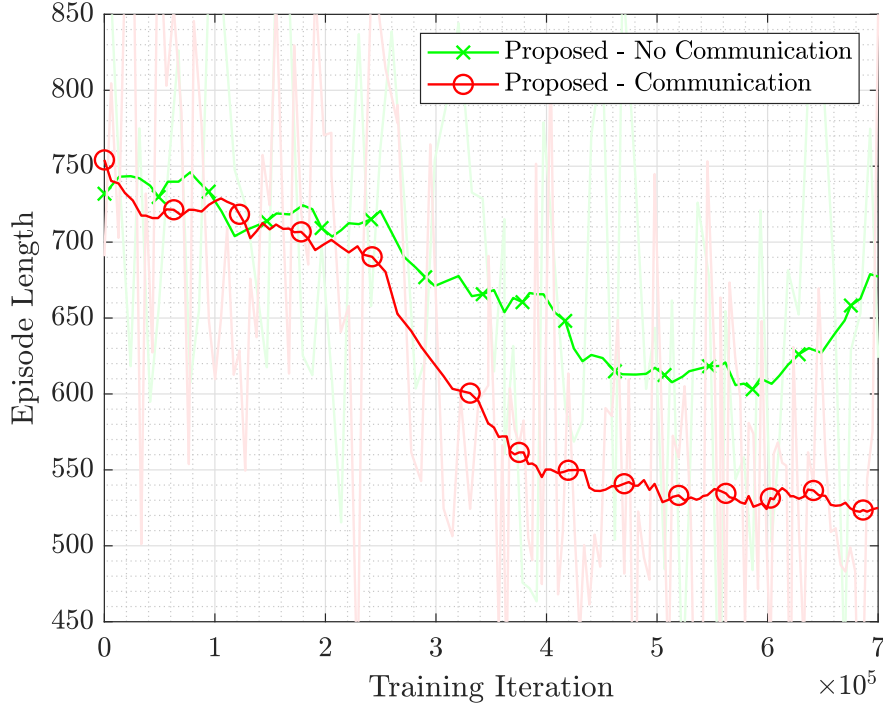


Figure 11: Episode length throughout training using the proposed method with and without communication.

shows the achieved performance where each point is the average over the evaluation episodes. Note that the policy is trained with an ideal transmission conditions, i.e., with $\beta = 0$. We observe that the trained policy generalizes well, with an acceptable degradation in performance even when $\beta = 0.5$.

E. Emergent communication

Finally, in order to detect whether communication has emerged at all during the training process, we train the same scenario without a communication channel and compare the achieved performance of both cases, i.e., with and without communication [31]. In Figs. 11, 12, and 13, we analyze the episode length, total reward, and the timeout achieved during the training process by the proposed method, with and without communication. We can see that when a communication channel exists among the agents, the performance is improved significantly. This corroborates the fact that when agents communicate, they can help each other to complete the task much better than working independently. It should be noted that at the beginning of the training, the

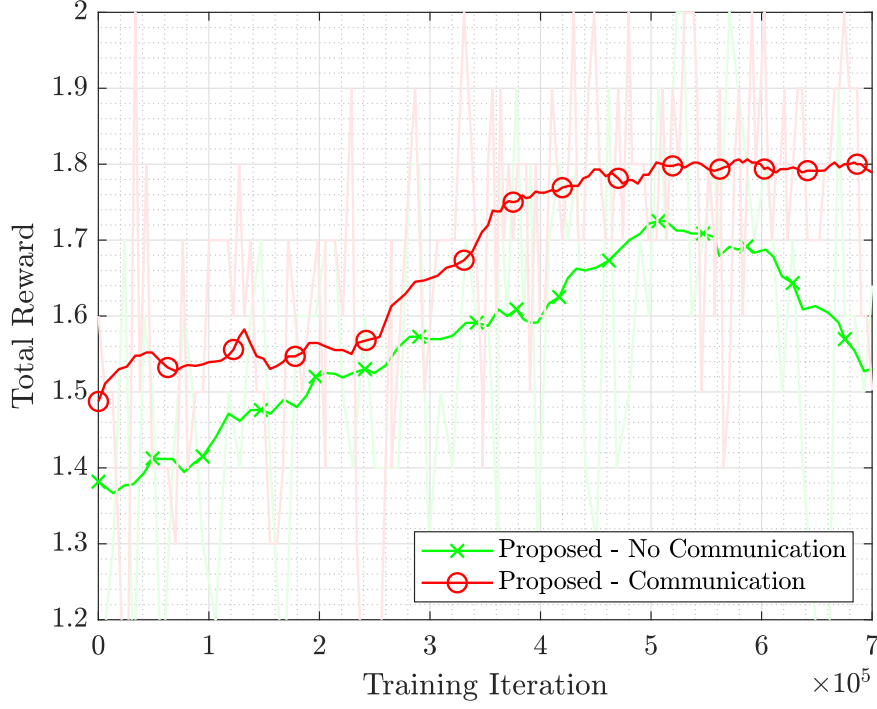


Figure 12: Total reward achieved by the agents throughout training using the proposed method with and without communication.

messages had no prior meaning while towards the end, a meaning has been emerged allowing both agents to cooperate well.

VI. CONCLUSION

In this work, we have proposed a novel adaptive state abstraction for a cooperative FoV-based navigation scenario. In particular, we proposed a neural network architecture to jointly learn an adaptive state space abstraction, along with a communication protocol among agents to enhance coordination and cooperation. The main objective of the abstractor is to reduce the size of the state space to be explored during training, without much degradation in the policy performance. Simulations have shown that the state space can be significantly decreases and hence the complexity of RL policy training, without sacrificing the performance. Moreover, it was shown that the trained policy can generalize to cases when the local observations are uncertain about up to 60% of its contents due to noise, distortions or obstructed views. Finally, it is shown that communication emerges during training which helps the agents to learn better

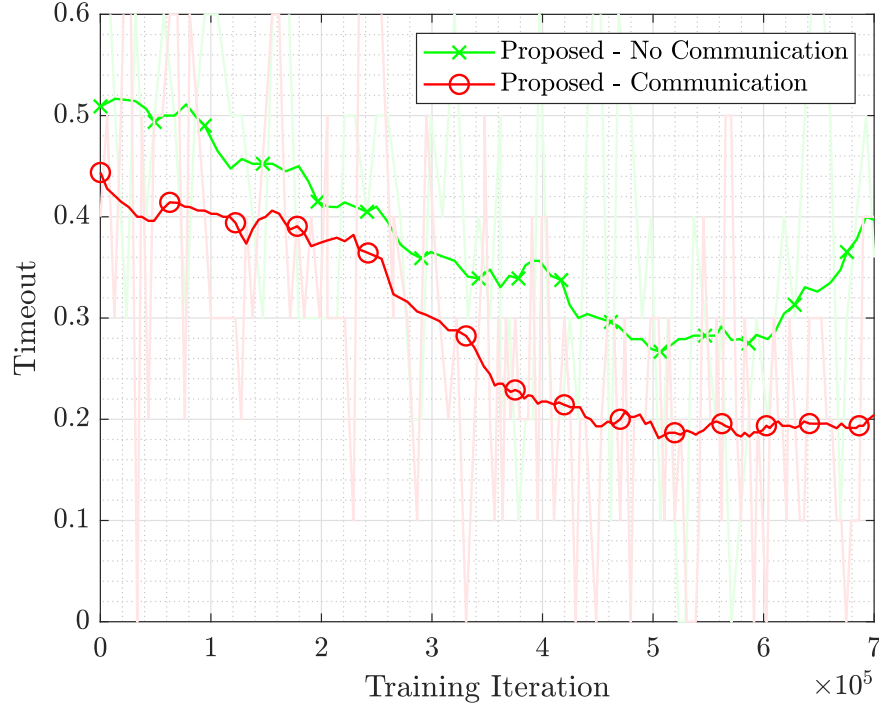


Figure 13: Timeout during the evaluation episodes throughout training using the proposed method with and without communication.

policies within fewer training iterations. Future work will aim at analysing the properties of the emerged communication protocol among the agents, as well as generalization to more agents.

REFERENCES

- [1] W. WEAVER, “Recent contributions to the mathematical theory of communication,” *ETC: A Review of General Semantics*, vol. 10, no. 4, pp. 261–281, 1953. [Online]. Available: <http://www.jstor.org/stable/42581364>
- [2] “Automated Guided Vehicle Market Size - Industry Report 2018-2024,” *GRAND VIEW RESEARCH*, Feb. 2018. [Online]. Available: <https://www.grandviewresearch.com/industry-analysis/automated-guided-vehicle-agv-market>
- [3] K. Zhu and T. Zhang, “Deep reinforcement learning based mobile robot navigation: A review,” *Tsinghua Science and Technology*, vol. 26, no. 5, pp. 674–691, Apr. 2021.
- [4] R. Mur-Artal, J. M. M. Montiel, and J. D. Tardós, “Orb-slam: A versatile and accurate monocular slam system,” *IEEE Transactions on Robotics*, vol. 31, no. 5, pp. 1147–1163, Oct. 2015.
- [5] G. Grisetti, C. Stachniss, and W. Burgard, “Improved techniques for grid mapping with rao-blackwellized particle filters,” *IEEE Transactions on Robotics*, vol. 23, no. 1, pp. 34–46, Feb. 2007.
- [6] M. Elbanhawi and M. Simic, “Sampling-based robot motion planning: A review,” *IEEE Access*, vol. 2, pp. 56–77, Jan. 2014.

- [7] Y. Zhu, R. Mottaghi, E. Kolve, J. J. Lim, A. Gupta, L. Fei-Fei, and A. Farhadi, "Target-driven visual navigation in indoor scenes using deep reinforcement learning," in *2017 IEEE International Conference on Robotics and Automation (ICRA)*, May 2017, pp. 3357–3364.
- [8] P. Mirowski, R. Pascanu, F. Viola, H. Soyer, A. J. Ballard, A. Banino, M. Denil, R. Goroshin, L. Sifre, K. Kavukcuoglu, D. Kumaran, and R. Hadsell, "Learning to navigate in complex environments," *CoRR*, vol. abs/1611.03673, Nov. 2016. [Online]. Available: <http://arxiv.org/abs/1611.03673>
- [9] V. Mnih, K. Kavukcuoglu, D. Silver, A. A. Rusu, J. Veness, M. G. Bellemare, A. Graves, M. Riedmiller, A. K. Fidjeland, G. Ostrovski *et al.*, "Human-level control through deep reinforcement learning," *nature*, vol. 518, no. 7540, pp. 529–533, Feb. 2015.
- [10] P. Hernandez-Leal, B. Kartal, and M. E. Taylor, "A survey and critique of multiagent deep reinforcement learning," *Autonomous Agents and Multi-Agent Systems*, vol. 33, no. 6, pp. 750–797, Oct. 2019.
- [11] L. Buşoniu, R. Babuška, and B. De Schutter, "Multi-agent reinforcement learning: An overview," in *Innovations in multi-agent systems and applications-1*. Springer, 2010, pp. 183–221.
- [12] H. Wang, W. Wang, X. Zhu, J. Dai, and L. Wang, "Collaborative visual navigation," *CoRR*, vol. abs/2107.01151, Jul. 2021. [Online]. Available: <https://arxiv.org/abs/2107.01151>
- [13] U. Jain, L. Weihs, E. Kolve, A. Farhadi, S. Lazebnik, A. Kembhavi, and A. G. Schwing, "A cordial sync: Going beyond marginal policies for multi-agent embodied tasks," *CoRR*, vol. abs/2007.04979, 2020. [Online]. Available: <https://arxiv.org/abs/2007.04979>
- [14] U. Jain, L. Weihs, E. Kolve, M. Rastegari, S. Lazebnik, A. Farhadi, A. G. Schwing, and A. Kembhavi, "Two body problem: Collaborative visual task completion," in *Proceedings of the IEEE/CVF Conference on Computer Vision and Pattern Recognition (CVPR)*, June 2019.
- [15] A. Valcarce and J. Hoydis, "Toward joint learning of optimal mac signaling and wireless channel access," *IEEE Transactions on Cognitive Communications and Networking*, vol. 7, no. 4, pp. 1233–1243, Dec. 2021.
- [16] J. Foerster, I. A. Assael, N. de Freitas, and S. Whiteson, "Learning to communicate with deep multi-agent reinforcement learning," in *Advances in Neural Information Processing Systems*, vol. 29. Curran Associates, Inc., 2016.
- [17] A. Lazaridou and M. Baroni, "Emergent multi-agent communication in the deep learning era," *CoRR*, vol. abs/2006.02419, Jul. 2020. [Online]. Available: <https://arxiv.org/abs/2006.02419>
- [18] S. S. Du, S. M. Kakade, R. Wang, and L. F. Yang, "Is a good representation sufficient for sample efficient reinforcement learning?" *CoRR*, vol. abs/1910.03016, 2019. [Online]. Available: <http://arxiv.org/abs/1910.03016>
- [19] T. Lin, J. Huh, C. Stauffer, S. N. Lim, and P. Isola, "Learning to ground multi-agent communication with autoencoders," in *Advances in Neural Information Processing Systems*, vol. 34, 2021, pp. 15 230–15 242.
- [20] J. Schulman, S. Levine, P. Abbeel, M. Jordan, and P. Moritz, "Trust region policy optimization," in *Proceedings of the 32nd International Conference on Machine Learning*, ser. Proceedings of Machine Learning Research, vol. 37. PMLR, Jul. 2015, pp. 1889–1897.
- [21] J. Schulman, F. Wolski, P. Dhariwal, A. Radford, and O. Klimov, "Proximal policy optimization algorithms," *CoRR*, vol. abs/1707.06347, 2017. [Online]. Available: <http://arxiv.org/abs/1707.06347>
- [22] D. Abel, D. Arumugam, K. Asadi, Y. Jinnai, M. L. Littman, and L. L. Wong, "State abstraction as compression in

- apprenticeship learning,” *Proceedings of the AAAI Conference on Artificial Intelligence*, vol. 33, no. 01, pp. 3134–3142, Jul. 2019.
- [23] M. Shanahan and M. Mitchell, “Abstraction for deep reinforcement learning,” *CoRR*, vol. abs/2202.05839, Apr. 2022. [Online]. Available: <https://arxiv.org/abs/2202.05839>
- [24] H. Samet, “The quadtree and related hierarchical data structures,” *ACM Comput. Surv.*, vol. 16, no. 2, pp. 187–260, Jun. 1984. [Online]. Available: <https://doi.org/10.1145/356924.356930>
- [25] M. L. Littman, “Markov games as a framework for multi-agent reinforcement learning,” in *Machine Learning Proceedings 1994*. Morgan Kaufmann, 1994, pp. 157–163.
- [26] L. Xu, D. Perez-Liebana, and A. Dockhorn, “Towards applicable state abstractions: a preview in strategy games,” in *The Multi-disciplinary Conference on Reinforcement Learning and Decision Making (RLDM)*, 2022.
- [27] K. Xu, W. Hu, J. Leskovec, and S. Jegelka, “How powerful are graph neural networks?” *CoRR*, vol. abs/1810.00826, Oct. 2018. [Online]. Available: <http://arxiv.org/abs/1810.00826>
- [28] E. Jang, S. Gu, and B. Poole, “Categorical reparameterization with gumbel-softmax,” *CoRR*, vol. abs/1611.01144, Nov. 2016. [Online]. Available: <https://arxiv.org/abs/1611.01144>
- [29] V. Mnih, A. P. Badia, M. Mirza, A. Graves, T. Lillicrap, T. Harley, D. Silver, and K. Kavukcuoglu, “Asynchronous methods for deep reinforcement learning,” in *Proceedings of The 33rd International Conference on Machine Learning*, ser. Proceedings of Machine Learning Research, vol. 48. PMLR, 20–22 Jun 2016, pp. 1928–1937. [Online]. Available: <https://proceedings.mlr.press/v48/mniha16.html>
- [30] D. P. Kingma and J. Ba, “Adam: A method for stochastic optimization,” *CoRR*, vol. abs/1412.6980, Dec. 2014. [Online]. Available: <https://arxiv.org/abs/1412.6980>
- [31] R. Lowe, J. N. Foerster, Y. Boureau, J. Pineau, and Y. N. Dauphin, “On the pitfalls of measuring emergent communication,” *CoRR*, vol. abs/1903.05168, Mar. 2019. [Online]. Available: <http://arxiv.org/abs/1903.05168>